A mixed-ligand Co(II) MOF synthesized from a single organic ligand to capture iodine and methyl iodide vapour

Yilong Lin,[a] Panyu Zeng,[a] Die Wang,[a] Tian-Tian Li,*[a] Liang-Hua Wu,[b] Sheng-Run Zheng*[b]

[a]College of Pharmacy, Guizhou University of Traditional Chinese Medicine Guiyang, Guizhou, 550002, P. R. China.

[b]School of Chemistry, South China Normal University, Guangzhou, 510006, P. R. China

*Corresponding author: Dr. Tian-Tian Li; Prof. Sheng-Run, Zheng

E-mail address: zhengsr@scnu.edu.cn; 525708251@qq.com

Tel./Fax.: +86-20-39310187

Supporting Information

Table S1 Crystallographic data and structure refinement summary for Co-IPT-IBA

Complex	Co-IPT-IBA
Empirical formula	$C_{20}H_{16}N_8O_4Co_2$
Formula weight	550.27
Crystal system	orthorhombic
Space group	*I*ba2
a / Å	25.418(13)
b / Å	32.433(16)
c / Å	6.875(4)
α / °	90
β / °	90
γ / °	90
V / Å^3	5667(5)
Z	88
D / g cm^{-3}	1.290
μ / mm^{-1}	1.206
T / K	293(2)
R^a / wR^b	0.0504/0.1054
Total / unique	6373/4331
Rint	0.0740

[a] $R_1 = \Sigma||F_o| - |F_c||/|F_o|$, [b] $wR_2 = [\Sigma w(F_o^2 - F_c^2)^2/\Sigma w(F_o^2)^2]^{1/2}$, where $w = 1/[\sigma^2(F_o^2) + (aP)_2 + bP]$. $P = (F_o^2 + 2F_c^2)/3$.

*The refinement results were obtained from squeeze data.

Table S2 Selected bond lengths [Å] and angles [°] for Co-IPT-IBA

Co-IPT-IBA			
Co(1)-O3	2.023(5)	Co(1)-O(2)#1	2.110(5)
Co(1)-N(5)#2	2.027(5)	Co(1)-N(4)#3	2.103(6)
Co(1)-O(2)	2.122(5)	Co(1)-N(8)#4	2.1132(5)
Co(2)-O(3)	2.070(4)	Co(2)-N(3)#5	2.336(7)
Co(2)-N(6)#2	2.398(7)	Co(2)-N(1)	2.068(5)
Co(2)-O(1)	2.015(4)	Co(2)-O(1W)	2.120(5)
O(3)-Co(1)-O(3)#1	167.56(13)	O(3)-Co(1)-N(5)#2	85.77(17)
Co(1)N(4)#3	91.2(2)	O(3)-Co(1)-O(2)	174.80(17)
O(3)#1Co(1)O(2)	83.30(17)	O(3)-Co(1)-N(8)#4	84.9(2)
O(3)#1-Co(1)-N(8)#4	106.4(2)	N(5)#2-Co(1)-O(3)#1	91.2(2)
N(5)#2-Co(1)-O(2)	83.2(2)	N(5)#2-Co(1)-N(8)#4	92.9(2)
N(4)#3-Co(1)-O(3)#1	83.3(2)	N(4)#3-Co(1)-N(5)#2	173.2(3)
N(4)#3-Co(1)-O(2)	92.1(2)	N(4)#3-Co(1)-N(8)#4	92.6(2)
O(2)-Co(1)-N(8)#4	169.6(2)	O(3)-Co(2)-N(3)#5	84.8(2)
O(3)-Co(2)-N(6)#2	93.4(2)	O(3)-Co(2)-O(1W)	88.64(17)
N(3)#5-Co(2)-N(6)#2	176.55(19)	N(1)-Co(2)-O(3)	177.9(3)
N(1)-Co(2)-N(3)#5	93.3(2)	N(1)-Co(2)-N(6)#2	88.5(2)
N(1)-Co(2)-O(1W)	90.4(2)	O(1)-Co(2)-O(3)	89.32(17)
O(1)-Co(2)-N(3)#5	99.16(19)	O(1)-Co(2)-N(6)#2	83.71(19)
O(1)-Co(2)-N(1)	91.76(19)	O(1)-Co(2)-O(1W)	175.1(2)
O(1W)-Co(2)-N(3)#5	85.1(2)	O(1W)-Co(2)-N(6)#2	91.9(2)

Symmetry transformations used to generate equivalent atoms: #1 3/2 - x, 1/2 - y, 1/2 + z; #2 x, 1 - y , 1/2 + z; #3 3/2 - x, -1/2 + y, z; #4 -1/2 + x, 1/2 - y, z; #5 x, 1 - y, -1/2 + .

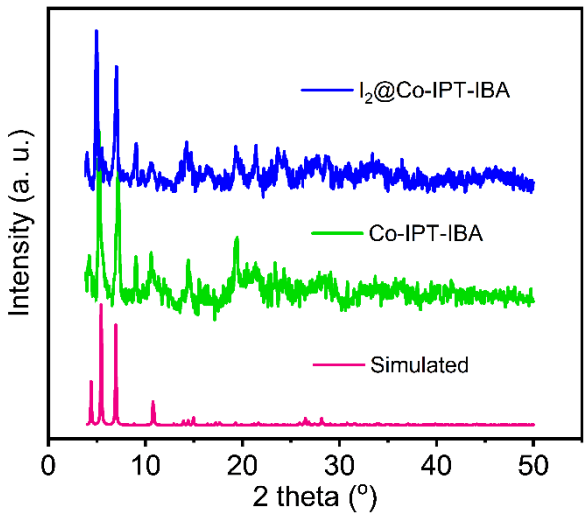

Fig. S1 The PXRD of the simulated, as-synthesized, and activated Co-IPT-IBA.

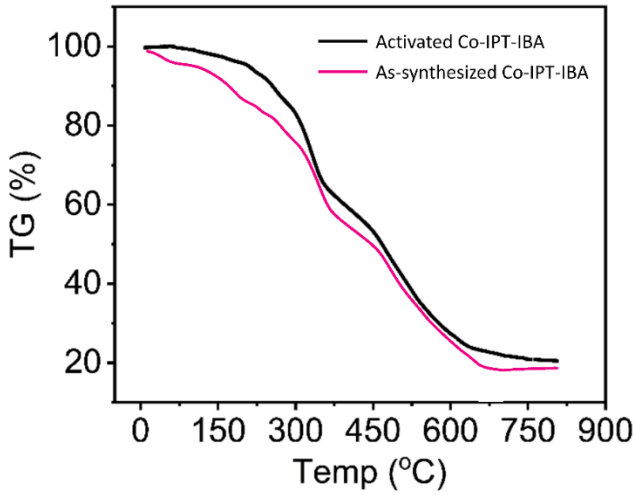

Fig. S2 The TG of the as-synthesized and activated Co-IPT-IBA.

Table S3. Iodine adsorption capacities via vapor diffusion at 75-85 °C in previous literature reports of MOF materials.

MOFs	Iodine uptake (g/g)	Reference
MIL-53-SH(Al)	0.33	S1
UiO-67	0.53	S2
UiO-66	0.66	S3
MOF-867	0.88	S2
MFM-300(Al)	0.94	S4
Th-UiO-66	0.97	S5
ZIF-8	1.25	S6
MFM-300(V^{III})	1.42	S4
NU-100	1.45	S2
HKUST-1	1.75	S7
MOF-808	2.18	S2
Cu-MIL-101	3.42	S8
MIL-101-ED (5 mmol)	4.37	S9
SCNU-Z7	2.7	S10
Co-IPT-IBA	2.88	This work

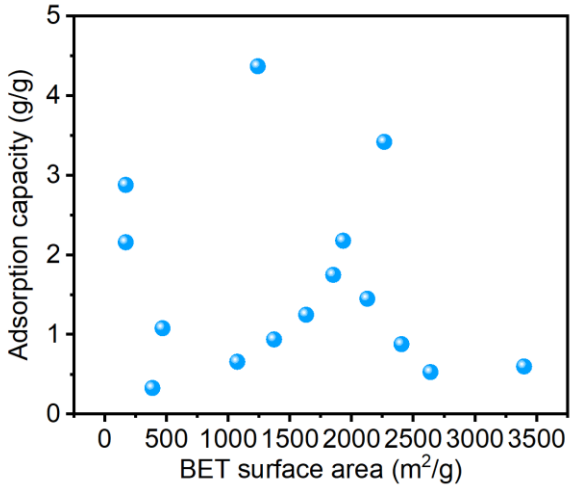

Fig. S3. Correlations of I_2 vapor adsorption uptake capacity with BET surface area in MOFs.

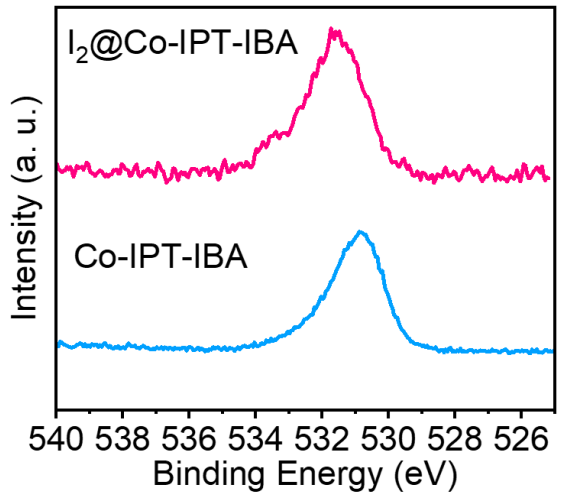

Fig. S4 The O_{1S} XPS of Co-IPT-IBA and I_2@Co-IPT-IBA.

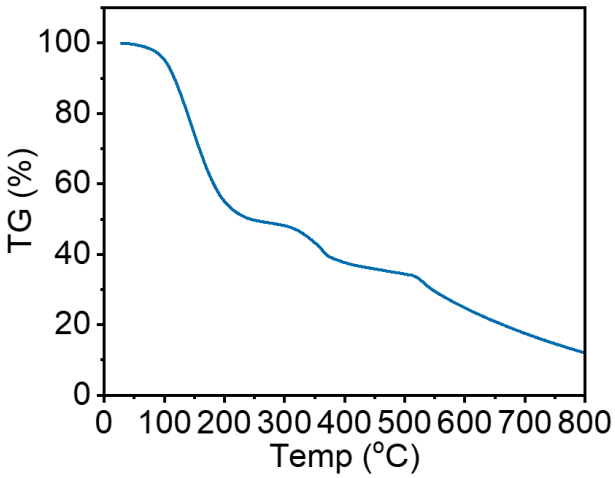

Fig. S5 The TG curve of I_2@Co-IPT-IBA.

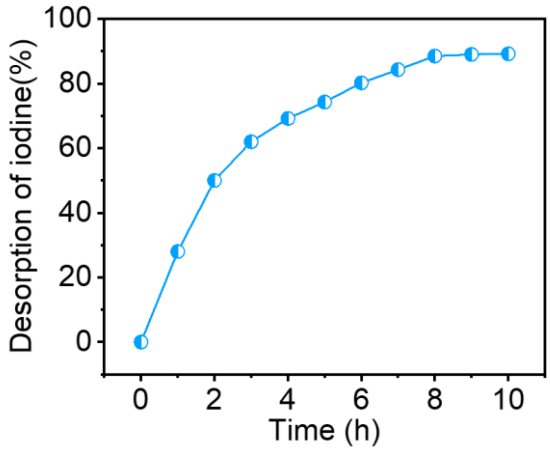

Fig. S6 The desorption of iodine on I_2@Co-IPT-IBA.

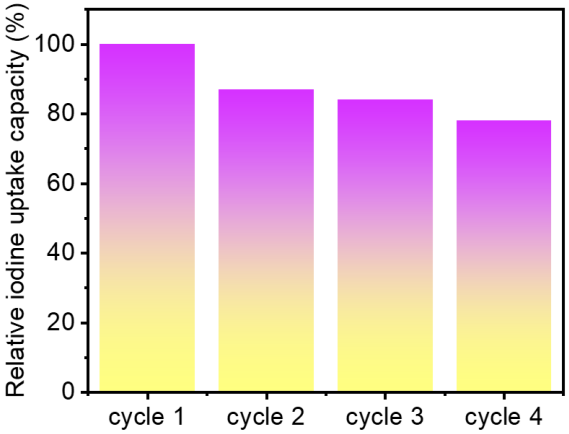

Fig. S7 Recycling efficiency of Co-IPT-IBA for I_2 vapor adsorption.

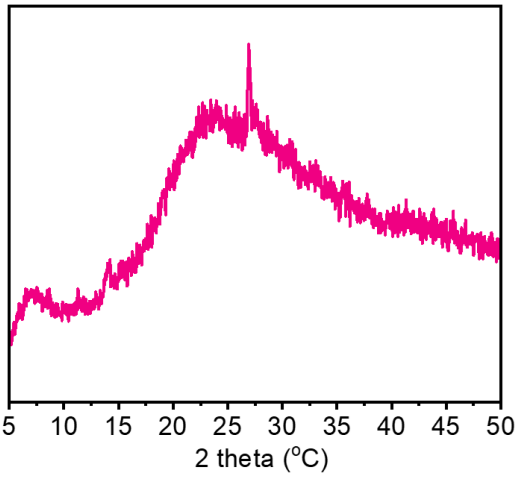

Fig. S8 The PXRD of CH_3I@Co-IPT-IBA.

Reference

S1. A. S. Munn, F. Millange, M. Frigoli, N. Guillou, C. Falaise, V. Stevenson, C. Volkringer, T. Loiseau, G. Cibinf and R. I. Walton, Iodine sequestration by thiol-modified MIL-53(Al), *CrystEngComm*, 2016, **18**, 8108–8114.

S2. P. Chen, X.-H. He, M.-B. Pang, X.-T. Dong, S. Zhao and W. Zhang, Iodine Capture Using Zr-Based Metal–Organic Frameworks (Zr-MOFs): Adsorption Performance and Mechanism, *ACS Appl. Mater. Inter*., 2020, **12**, 20429–20439.

S3. J. Maddock, X.-C. Kang, L.-F. Liu, B.-X. Han, S.-H. Yang and M. Schröder, The Impact of Structural Defects on Iodine Adsorption in UiO-66, *Chemistry*, 2021, **3**, 525–531.

S4. X.-R. Zhang, I. da Silva, H. G. W. Godfrey, S. K. Callear, S. A. Sapchenko, Y. Q. Cheng, I. Vitórica-Yrezábal, M. D. Frogley, G. Cinque, C. C. Tang, C. Giacobbe, C. Dejoie, S. Rudić, A. J. Ramirez-Cuesta, M. A. Denecke, S.-H. Yang and M. Schröder, Confinement of Iodine Molecules into Triple-Helical Chains within Robust Metal–Organic Frameworks, *J. Am. Chem. Soc.*, 2017, **139**, 16289–16296.

S5. Z.-J. Li, Y. Ju, H.-J. Lu, X.-L. Wu, X.-L. Yu, Y.-X. Li, X.-W. Wu, Z.-H. Zhang, J. Lin, Y. Qian, M.-Y. He and J.-Q. Wang, Boosting the Iodine Adsorption and Radioresistance of Th-UiO-66 MOFs via Aromatic Substitution, *Chem. Eur. J.*, 2021, **18**, 1286−1291.

S6. T. D. Bennett, P. J. Saines, D. A. Keen, J.-C. Tan and A. K. Cheetham, Ball-Milling-Induced Amorphization of Zeolitic Imidazolate Frameworks (ZIFs) for the Irreversible Trapping of Iodine, *Chem. Eur. J.*, 2013, **19**, 7049–7055.

S7. D. F. Sava, K. W. Chapman, M. A. Rodriguez, J. A. Greathouse, P. S. Crozier, H.-Y. Zhao, P. J. Chupas and T. M. Nenoff, Competitive I_2 Sorption by Cu-BTC from Humid Gas Streams, *Chem. Mater*., 2020, **238**, 116488.

S8. B.-B. Qia, Y. Liu, T. Zheng, Q.-H. Gao, X.-W. Yan, Y. Jiao and Y. Yang, Highly efficient capture of iodine by Cu/MIL-101, *J. Solid State Chem.*, 2018, **258**, 49–55.

S9. P. Tang, X.-X. Xie, Z.-Y. Huang, X.-T. Cai, W.-G. Zhang, S.-L. Cai, J. Fan and S.-R. Zheng, Ethylenediamine grafted MIL-101 for iodine vapor capture with high capacity, *J. Solid State Chem*., 2022, **315**, 123453.

S10. J. Y. Xian, X. X. Xie, Z. Y. Huang, Y. L. Liu, H. Y. Song, Z. Q. Chen, Y. C. Ou and Sheng-Run Zheng, Structure and Properties of a Mixed-Ligand Co-MOF That Was Synthesized in Situ from a Single Imidazole-Pyridyl-Tetrazole Trifunctional Ligand, *Cryst. Growth Des.*, 2023, **23**, 1448–1454.